Acta Oceanologica Sinica, Vol. 11, No. 1, pp. 13~23, 1992. ISSN 0253-505X
Published by China Ocean Press.

LAGFD-WAM numerical wave model— Ⅱ.

Characteristics inlaid scheme and its application

Yuan Yeli,[1] Hua Feng,[1] Pan Zengdi[1] and Sun Letao[1]

(*Received October* 24,1990; *accepted August* 15 , 1991)

Abstract——In this paper the parameterizational approach of nonlinear source function and the implicit scheme of the model are discussed in detail. The matching problem is solved between time and space steps using the characteristics inlaid scheme with very strong physical meaning. The computational comparison in typical winds shows some improvements to the WAM model. That the hindcast results of the model for typhoon cases are in good agreement with real data illustrates its applicability to wave forecast and engineering study.

INTRODUCTION

In the paper "LAGFD-WAM model— I ", we have pointed out that the main properties of the model are : i) the dispersion of the wave energy packet base is considered in derivation of the energy spectrum balance equaton; ii) the physical model is quite complete, which includes all the useful results of wave theory and experiment such as the input source function, the nonlinear interaction function, the improved breaking dissipation function, the improved bottom friction function and the wave-current interaction function; iii) in the complicated characteristics equations derived, the effect of unsteady ambient fields on wave propagation is considered, this is a more realistic presentation. In the second section of this paper, the basic configuration of the characteristics inlaid scheme will be given, in the third and forth sections we shall expound the parameterization of the nonlinear source function in wave-number space and the implicit scheme approach of the model respectively. In the fifth we shall make a comparison between two kinds of computations for the model: one is with the WAM model in three typical wind fields: parallel, turning and rotating, the other is with the measured data of the typhoon sea.

THE CHARACTERISTICS INLAID SCHEME

In previous paper (Yuan *et al.* , 1990), we have derived the governing equations of the LAGFD-WAM model as follows:

i)
$$\left[\frac{\partial}{\partial t} + \boldsymbol{C}_g + \boldsymbol{U}) \nabla \right] E(\boldsymbol{k}) = S_{\text{in}}(\boldsymbol{k}) + S_{\text{nl}}(\boldsymbol{k}) + S_{\text{ds}}(\boldsymbol{k}) + S_{\text{cu}}(\boldsymbol{k}) = SS(\boldsymbol{k}), \quad (1)$$

1. First Institute of Oceanography, State Oceanic Administration, Qingdao 266003, China

ii) $$\frac{dX}{dt} = (C_g + U), \tag{2}$$

iii) $$\left[\frac{\partial}{\partial t} + (C_g + U)\nabla\right]K = -\left[\frac{\partial\omega}{\partial D}\frac{\partial D}{\partial s} + KL_1\frac{\partial U}{\partial s}\right], \tag{3}$$

iv) $$\left[\frac{\partial}{\partial t} + (C_g + U)\nabla\right]\theta_1 = -\frac{1}{K}\left[\frac{\partial\omega}{\partial D}\frac{\partial D}{\partial n_1} + KL_1\frac{\partial U}{\partial n_1}\right]. \tag{4}$$

All the equations have physical meaning of the wave packet propagation along a ray, so in order to reflect this property, it is necessary to design a characteristics inlaid computation scheme. It is of great benefit to deal with the fine grid embedment and the earth surface curvature.

The basic computational configuration of the LAGFD-WAM model is as Fig. 1.

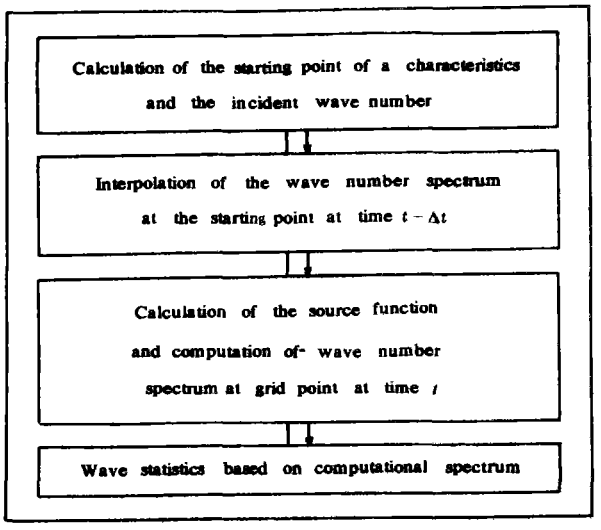

Fig. 1. The computation configuration of the LAGFD-WAM model.

Grid distribution in physical and phase spaces

In physical space, the grid points are distributed according to the accuracy requirement of different area and the convenience of interpolation. In general we take the grid parallel to the longitute and latitude lines.

In wave-number space, we take polar coordinate grids with $(n+1)\times m$ cross-points.

In consideration of the inhomogeneity of the spectrum distribution: sharp in low frequency domain and smooth in high frequency domain, the division of wave-number mode is taken as below:

$$K(\alpha) = K_{\min}\exp\{(\alpha - 1)\triangle K\}. \qquad \alpha = 1, \cdots, n+1, \tag{5}$$

where $K_{\min} = 0.0071$ is the minimum divisional mode and $K_{\max} = 0.6894$ is the maximum one and

$$\triangle K \equiv \frac{1}{n}\ln\frac{K_{\max}}{K_{\min}}. \tag{6}$$

The incident wave direction division at grid point is taken as homogeneous as below:

$$\theta_1(\beta) = \theta(\beta) + \pi, \tag{7}$$

where $\theta(\beta) = (\beta - 1)\triangle\theta, \beta = 1, \cdots, m$, and

$$\triangle\theta = \frac{2\pi}{m}. \tag{8}$$

In the division above n and m are values according to the requirement of computational accuracy and speed.

The computation of the segments of the characteristics set

At each grid point in physical space, there are $(n+1) \times m$ characteristics segments. The starting point of a segment is indicated as $(X_0, K_0(\alpha), \theta_{10}(\beta))$ and the ending point as $(X, K(\alpha), \theta_1(\beta))$. The latter is the divisional wave number at grid point, and the former is the location and wave number of incident wave packet at time $t - \triangle t$. They can be determined by the following equations:

$$x_0 = x - [C_g(K(\alpha))\cos\theta_1(\beta) + U_1]\triangle t, \tag{9}$$

$$y_0 = x - [C_g(K(\alpha))\sin\theta_1(\beta) + U_2]\triangle t, \tag{10}$$

$$K_0(\alpha) = K(\alpha) + (\frac{\partial\omega}{\partial D}\frac{\triangle D}{\triangle s} + K(\alpha)L_1\frac{\triangle U}{\triangle s})\triangle t, \tag{11}$$

$$\theta_{10}(\beta) = \theta_1(\beta) + \frac{1}{K(\alpha)}\left(\frac{\partial\omega}{\partial D}\frac{\triangle D}{\triangle n_1} + K(\alpha)L_1\frac{\triangle U}{\triangle n_1}\right)\triangle t, \tag{12}$$

where $L_1 = \cos(\theta_1(\beta))\mathbf{i} + \sin(\theta_1(\beta))\mathbf{j}$ is the wave direction which is not consistent with that of $X - X_0$ in general, and $\triangle/\triangle s$ is the derivative along L_1 at X or X_0, $\triangle/\triangle n_1$ is that along 90° turning of L_1 at X or X_0.

The interpolation of spectrum $E(K_0, \theta_{10}; X_0; t - \triangle t)$

Obviously $K_0 = (K_0(\alpha), \theta_{10}(\beta))$ and $X_0 = X - (Cg + U)\triangle t$ will fall in the grids consisting of the points $\{[K_0/\triangle K] + 1\}$ and $\triangle K[K_0/\triangle K]\triangle K$ and $\{[X_0/\triangle X] + 1\}\triangle X$ and $[X_0/\triangle X]\triangle X$ respectively.

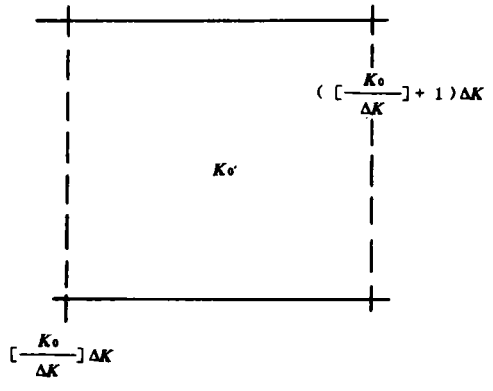

Fig. 2. Grid in wave-number space.

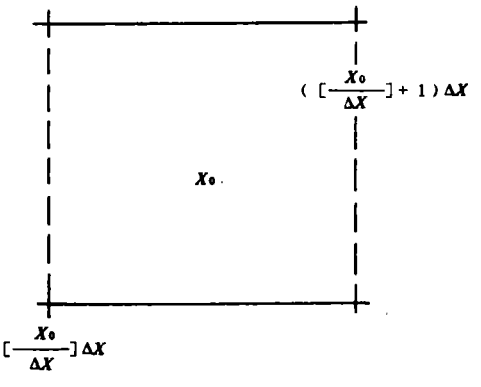

Fig. 3. Grid in physical space.

The steps of the interpolation are:

(1) at each point of $[X_0/\triangle X]\triangle X$ and $([X_0/\triangle X] + 1)\triangle X$ in grid consisting of

$[\boldsymbol{K}_0/\triangle\boldsymbol{K}]\triangle\boldsymbol{K}$ and $([\boldsymbol{K}_0/\triangle\boldsymbol{K}]+1)\triangle\boldsymbol{K}$ to interpolate $E(\boldsymbol{K}_0, t-\triangle t)$ by using $E(t-\triangle t)$; (2) in the grid consisting of $[\boldsymbol{X}_0/\triangle\boldsymbol{X}]\triangle\boldsymbol{X}$ and $([\boldsymbol{X}_0/\triangle\boldsymbol{X}]+1)\triangle\boldsymbol{X}$ to interpolate $E(\boldsymbol{K}_0, \boldsymbol{X}_0; t-\triangle t)$ by using $E(\boldsymbol{K}_0, t-\triangle t)$.

In the interpolation process, the double linear interpolation formula is used as follows:

$$E(A,B)=\sum_{i,j=1}^{2}E(A_i,B_j)\psi_{ij}(A,B), \tag{13}$$

where $\psi_{ij}(A,B)$ is the rectangle or trapezoid interpolation function.

THE PARAMETERIZED COMPUTATION OF THE NONLINEAR INTERACTION SOURCE FUNCTION

In order to avoid the calculation of the 6-D Boltzman integral it is necessary to simplify the computation by parameterization. On the basis of a vast amount of computation test, Hasselmann (1985) pointed out: i) the main properties of the exact nonlinear source function can be calculated on a pair of interaction configurations consisting of neighbour wave and finite-divided waves, ii) the interaction configurations satisfy the following condition:

a)

$$\boldsymbol{k}_1=\boldsymbol{k}_2=\boldsymbol{k}, \quad \text{and } \omega_1=\omega_2=\omega, \tag{14}$$

here $\boldsymbol{k}_1$ is the computed wave, $\boldsymbol{k}_2$ is the neighbour wave.

b) In order to satisfy the resonance condition $\omega_1+\omega_2-\omega_3-\omega_4=0$, we take

$$\omega_3=(1+\lambda)\omega, \tag{15}$$

$$\omega_4=(1-\lambda)\omega, \tag{16}$$

and

$$\lambda=0.25, \tag{17}$$

and the wave modes are

$$K_3=(1+\lambda)^2K, \quad K_4=(1-\lambda)^2K. \tag{18}$$

c) In order to satisfy the resonance condition $\boldsymbol{k}_1+\boldsymbol{k}_2-\boldsymbol{k}_3-\boldsymbol{k}_4=0$, the angles of $\boldsymbol{k}_3$ to $\boldsymbol{k}$ and $\boldsymbol{k}_4$ to $\boldsymbol{k}$ are

$$\theta_3=11.5^\circ \text{ and } \theta_4=-33.6^\circ, \tag{19}$$

respectively. In the following we indicate

$$\boldsymbol{k}_1=\boldsymbol{k}_2=\boldsymbol{k}, \quad \boldsymbol{k}_3=\boldsymbol{k}_+, \quad \boldsymbol{k}_4=\boldsymbol{k}_-. \tag{20}$$

The other interaction configuration of the pair is the symmetric image of the above one about the $\boldsymbol{k}$-axis. In this case in the time interval $\triangle t$, the variation of action spectrum of each wave packet of an interaction configuration can be written as

$$\begin{Bmatrix}\delta N\\ \delta N_+\\ \delta N_-\end{Bmatrix}=\begin{Bmatrix}-2\\ 1\\ 1\end{Bmatrix}c'\frac{g^{-8}\omega^{19}}{(2\pi)^{19}}[N^2(N_++N_-)-2NN_+N_-]\triangle\boldsymbol{k}\triangle t. \tag{21}$$

The corresponding increments of the nonlinear source function in wave-number space are

$$\begin{Bmatrix}\delta S_{nl}\\ \delta S_{nl+}\\ \delta S_{nl-}\end{Bmatrix} \equiv \frac{1}{\Delta t}\begin{Bmatrix}\omega\dfrac{\delta N}{\Delta k}\\ \omega_+\dfrac{\delta N_+}{\Delta k_+}\\ \omega_-\dfrac{\delta N_-}{\Delta k_-}\end{Bmatrix}$$

$$= \begin{Bmatrix}-2\omega\dfrac{\Delta k}{\Delta k}\\ \omega_+\dfrac{\Delta k}{\Delta k_+}\\ \omega_-\dfrac{\Delta k}{\Delta k_-}\end{Bmatrix} c'\frac{g^{-8}\omega^{19}}{(2\pi)^{19}}[N^2(N_+ + N_-) - 2N\,N_+N_-]$$

$$= \begin{Bmatrix}-2\\ \dfrac{1}{(1+\lambda)^3}\\ \dfrac{1}{(1-\lambda)^3}\end{Bmatrix} c'\frac{g^{-8}\omega^{17}}{(2\pi)^{-19}}\left[E^2\left(\frac{E_+}{1+\lambda}+\frac{E_-}{1-\lambda}\right) - 2\frac{E\,E_+E_-}{1-\lambda^2}\right]$$

$$= \begin{Bmatrix}-2\\ \dfrac{1}{(1+\lambda)^3}\\ \dfrac{1}{(1-\lambda)^2}\end{Bmatrix} C_L g^{1/2}K^{17/2}\left[E^2\left(\frac{E_+}{1+\lambda}+\frac{E_-}{1-\lambda}\right) - 2\frac{EE_+E_-}{1-\lambda^2}\right], \tag{22}$$

where C_L is the parameterization fitting coefficient. Taking Hasselmann's testing results we got

$$C_L \approx 7.86.$$

For discretization of the source function we take k the discrete point (the divisional wave number) and calculate the increments of the source function at each point k, k_+ and k_- first, then concentrate all the increments to the nearby discrete point and get the discrete nonlinear interaction source function. Obviously the integral of this function in wave-number space is zero:

$$\sum_k (\delta S_{nl} + \delta S_{nl+} + \delta S_{nl-}) = 0. \tag{23}$$

THE LAGFD-WAM IMPLICIT SCHEME

The energy spectrum balance equation can be divided into two parts of successive integrations.

i) The propagation equation

$$(C_g + U)\nabla E(k) = 0, \tag{24}$$

whose difference form is

$$E_i(K, X, t - \Delta t) = E(K_0, X_0, t - \Delta t_0). \tag{25}$$

where the right hand part $E(K_0, X_0, t - \Delta t_0)$ is the spectrum of time $t - \Delta t$ at the starting point of a characteristics segment.

ii) The local variation equation

$$\frac{\partial E(k)}{\partial t} = SS(k), \tag{26}$$

whose difference form is

$$\frac{E(\boldsymbol{K},\boldsymbol{X},t)-E_i(\boldsymbol{K},\boldsymbol{X},t-\triangle t)}{\triangle t}=SS\left[\frac{E(\boldsymbol{K},\boldsymbol{X},t)-E_i(\boldsymbol{K},\boldsymbol{X},t-\triangle t)}{2}\right]$$

$$=SS(E_i)+\frac{\partial SS(E_i)}{\partial E}\frac{(E-E_i)}{2}, \tag{27}$$

then we have the computation equation

$$E(\boldsymbol{K},t)\left[1-\frac{\triangle t}{2}\frac{\partial SS(E_i)}{\partial E}\right]=E_i\left[1-\frac{\triangle t}{2}\frac{\partial SS(E_i)}{\partial E}\right]+\triangle tSS(E_i)$$

or

$$E(X,K,t)=E_i+\frac{\triangle tSS(E_i)}{1-\frac{\triangle t}{2}\frac{\partial SS(E_i)}{\partial E}}. \tag{28}$$

In practical computation we take the implicit form Eq. (28) as $1-\frac{\triangle t}{2}\frac{\partial SS(E_i)}{\partial E}>1$, and otherwise the explicit form as follows:

$$E(\boldsymbol{X},\boldsymbol{K},t)=E_i+\triangle tSS(E_i). \tag{29}$$

The above computation approach is called half-implicit scheme.

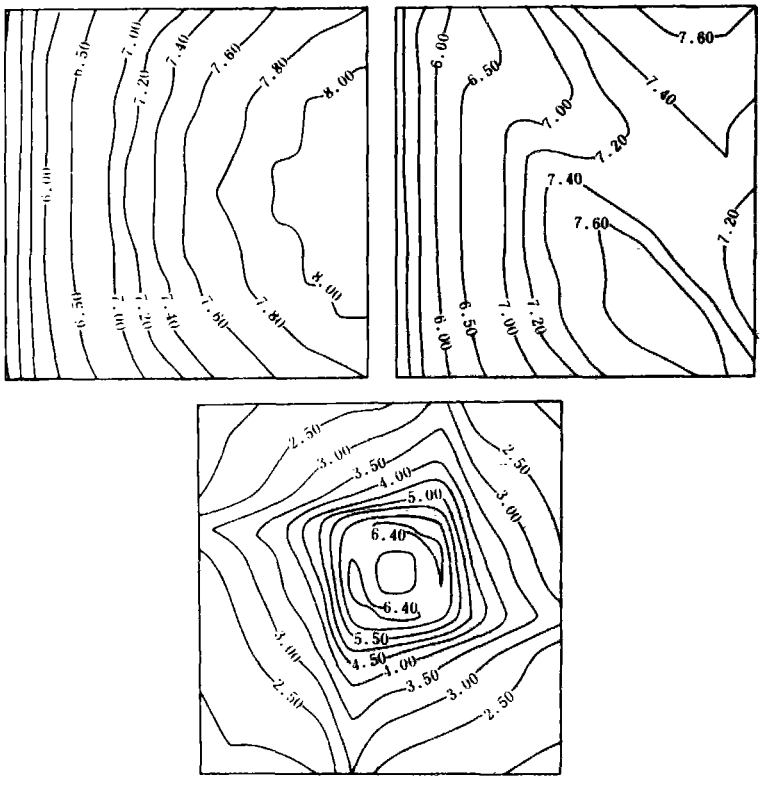

Fig. 4. Significant wave height by WAM model for uniform wind, turning wind and rotatory wind (after 40 h).

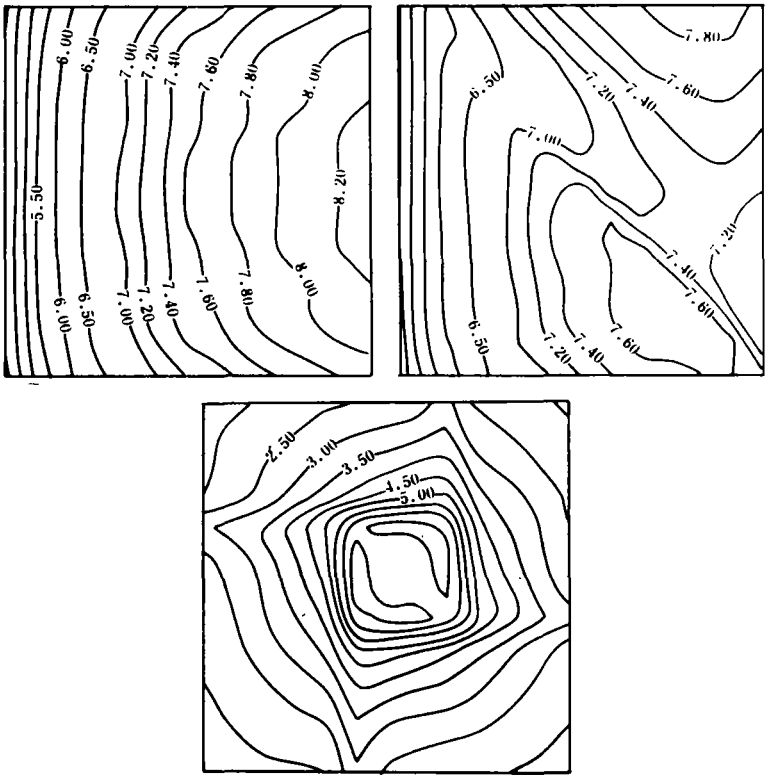

Fig. 5. Significant wave height by LAGFA model for uniform wind, turning wind and rotatory wind (after 40 h).

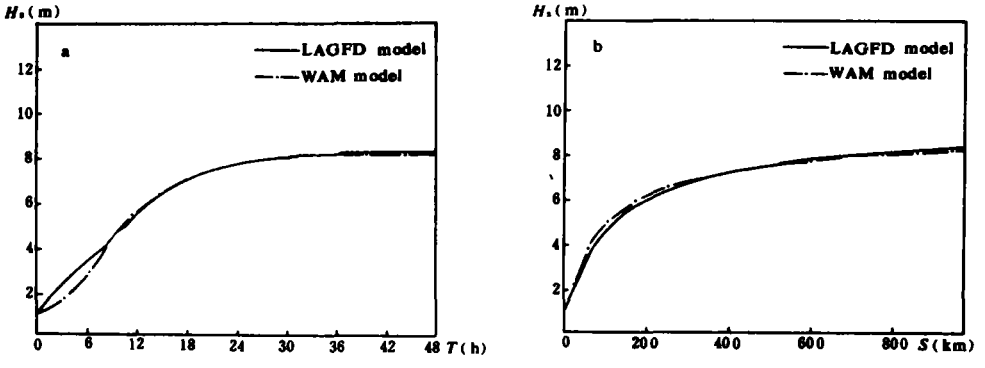

Fig. 6. Significant wave height as a function of time (a) and fetch (b) for uniform wind which speed is 20 m/s.

From Eq. (24) or (25) we know that the first term E_1 of Eqs (28) and (29) results from wave packet propagation, the second term $\triangle E$ is generated by all the source functions. In consideration of the Phillips' (1985) saturated spectrum limitation this part of the spectrum has to be less than $\triangle E_p$:

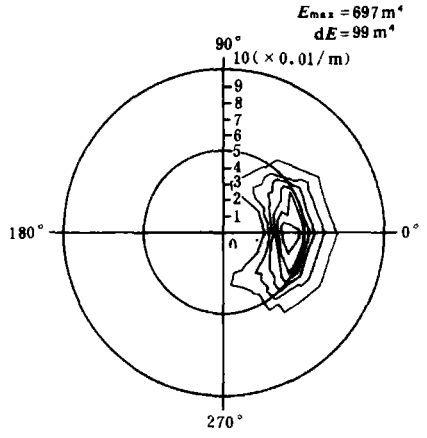

Point: A, wind direction: W

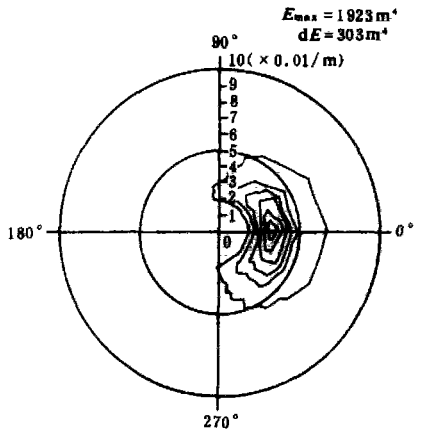

Point: B, wind direction: W

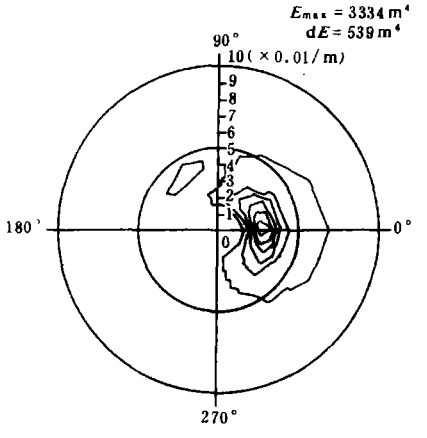

Point: C, wind direction: W

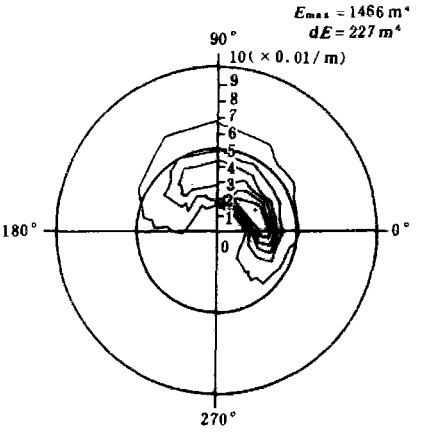

Point: D, wind direction: S

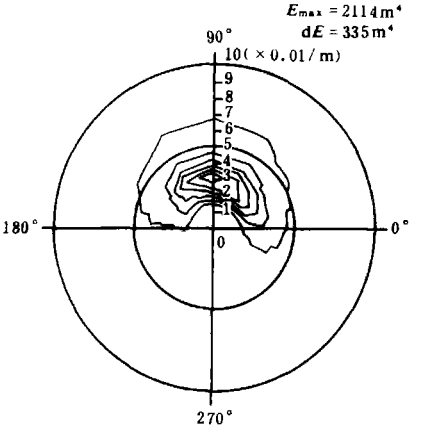

Point: E, wind direction: S

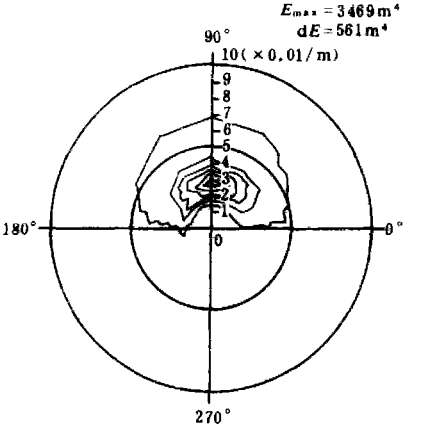

Point: F, wind direction: S

Fig. 7. Sequence of 2-D wave number spectra for turning wind which speed is 20 m/s.

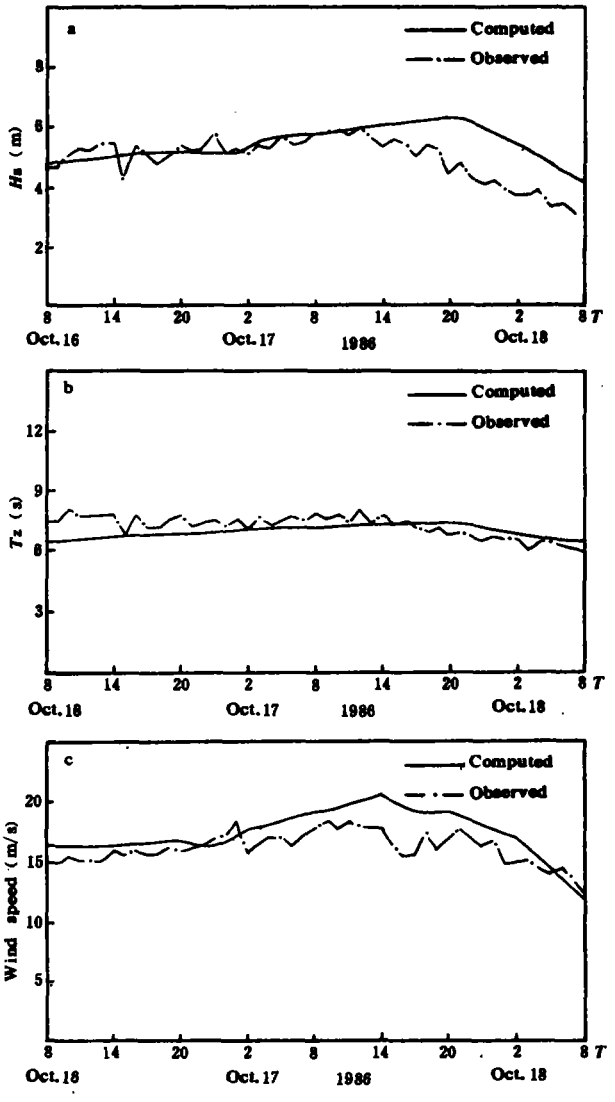

Fig. 8. Comparison between computed and observed values during Typhoon 8621 (Ellen) at the point of 21°30′ N and 115°30′ E.

$$\triangle E_p = p\cos^2(\theta_1 - \theta)H[\cos(\theta_1 - \theta)]\frac{u_*}{c}K^{-4}, \tag{30}$$

then we have

$$\triangle E = \min\{\triangle E, \triangle E_p\}. \tag{31}$$

EXPERIMENTS COMPARISON

In order to examine the correctness and the applicability of the LAGFD-WAM model, we carry out two kinds of numerical experiments and make a comparison between them.

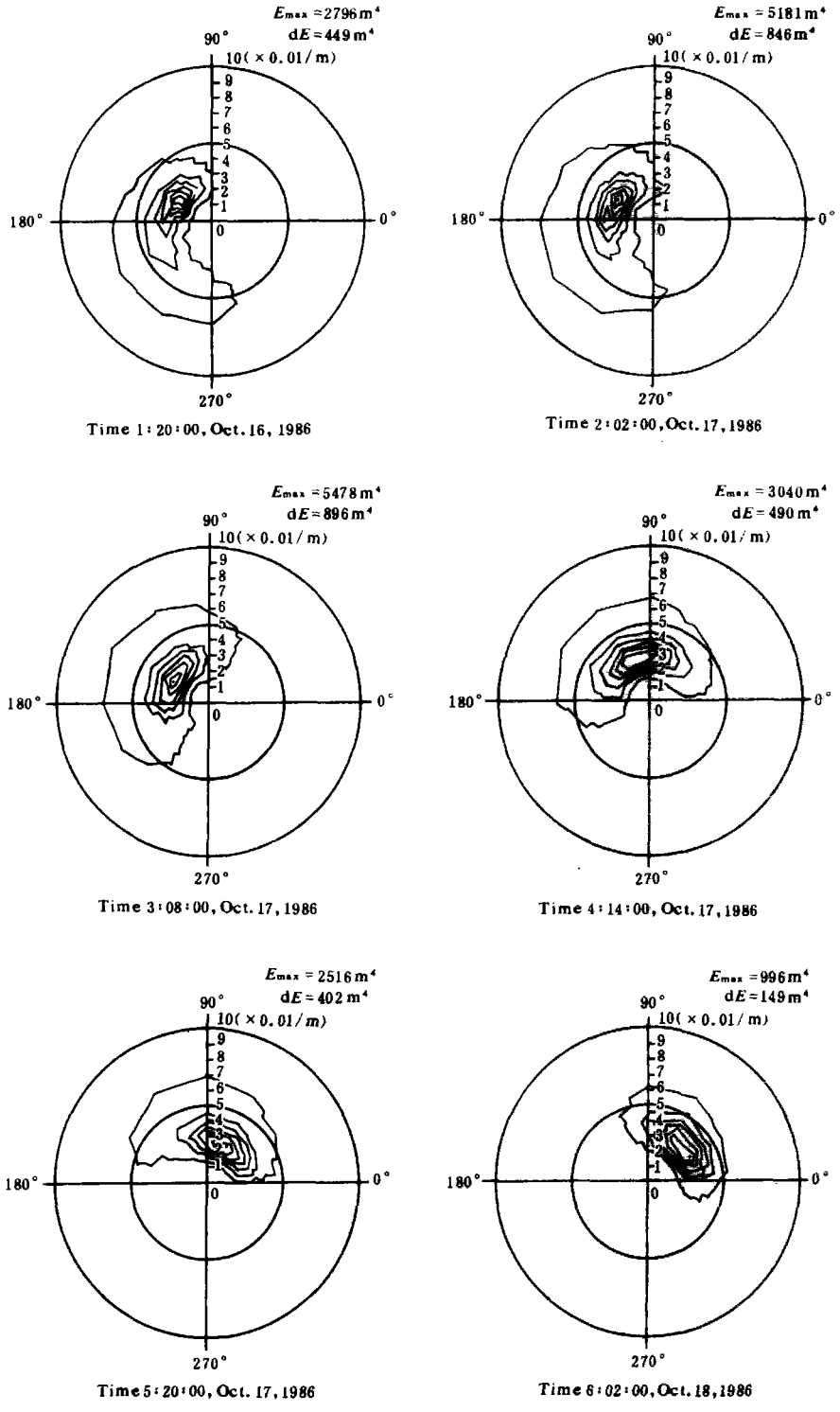

Fig. 9. Sequence of 2-D wave number spectra at the point of 20°30′ N and 115°30′ E during Typhoon 8621 (Ellen).

Comparison with the WAM model in three standard winds

In SWAMP (1985) project, three standard wind fields were suggested to test a wave model. In our comparison the parallel wind is $w = 20$ m/s; the turning wind direction is changed northward above the diagonal of northwest to southeast, and the rotation wind is the standard typhoon wind field such as that given by Jelesnianski(1966).

All the comparisons show good agreement of wave height distribution with that of the WAM model (see Figs 4 and 5), but the LAGFD-WAM model has more reasonable initial growth curve (see Fig. 6) and higher wave height in latter time. This is a good improvement to the WAM model.

In Fig. 7 we show the spectrum variation along the central line of the turning wind field and it shows that our model describes the spectrum movement very well and has good ability for spectral expression.

The comparison of the hindcast results with the field data

We take typhoon waves as an example to examine the applicability of the LAGFD-WAM model in the real sea. Because of the difficulties of the typhoon sea measurement by now, we just have a few of data series obtained by Merax buoy in strong sea state.

In Table 1 the basic parameters of typhoon Ellen (1986) is given, and in Fig. 8 the hindcast evolution curves of wave height (H_s) and period (T_s) are compared with real data. The results show that they have the same tendency and good agreement in quantity.

In Fig. 9 we show the variation process of the wave spectrum when the typhoon passed and left to the measured point. As the typhoon moved towards the point we had east wind and westerly waves, as the typhoon passed and left to the point we had southeast wind and northwesterly waves and after the typhoon we had southwest wind and northeasterly waves. The fact shows that our model has very good expression ability in directional wave spectrum.

REFERENCES

The WAMDI Group (1988) The WAM model—a third generation ocean wave prediction model. *J. Phys. Oceanogr.*, **18**, 1775～1810.

Yuan Yeli *et al.* (1990) LAGFD-WAM numerical wave model— I . Basic physical model. *Acta Oceanologica Sinica*, **10**, 483～488.

Yuan Yeli *et al.* (1990) (in press) Modern methods of numerical wave modelling computational physics series: Computational Oceanographic Physics, Hunan Sci. and Tech. Press.

Hasselmann S. *et al.* (1985) Computations and parameterizations of the nonlinear energy transfer in a gravity-wave spectrum, Part **I**. *J. Phys. Oceanogr.*, **15**, 1378～1390.

Phillips O. M. (1985) Spectral and statistical properties of equilibrium range in wind-generated gravity waves. *J. Fluid Mech.*, **156**, 505～531.

The SWAMP Group (1985) *Ocean Wave Modeling*, Plenum Press, 256pp.